

Abstract

We present a novel formulation, called the WaMPDE, for nonlinear systems driven

to voltage-controlled oscillators demonstrate speedups of two orders of magnitude.

1 Introduction

Nonlinear systems driven



Figure 1

form $x(t) = A \cos(\omega t + \phi)$

the separation of the time scales is often reduced artificially to make the problem tractable. As illustrated in Section 5, such ad-hoc approaches can lead to qualitatively misleading results.

The warped-time approach presented in

for autonomous systems with widely separated time scales. Earlier ef-

orts to generalize the MPDE to autonomous systems used non-rectangular boundaries to capture frequency

however, that this approach is limited to that eventually become and cannot, for instance, accommo-

3 Essential concepts

In this section, we introduce several concepts at the core of this work.

The remainder of this paper is organized as follows. Section 2 contains a brief review of previous work. Section 3 is a tutorial-style exposition of the main concepts. Section 4 presents the WaMPDE formulation, the mathematical details of which are presented in Section 4. In Section 5, the new methods are applied to practical VCO circuits and compared against existing techniques.

2 Previous Work

Most previous analyses of oscillators have typically apply purely linear models to obtain simple design formulae. Nonlinear analytical studies have largely been of limited use.

For real oscillators, numerical simulation has been the predominant means of predicting detailed responses. A fundamental problem, however, is the intrinsic phase-instability of oscillators, leading to unbounded increase in phase error during simulation. Boundary-value methods like shooting (e.g., [1])

a two-tone quasiperiodic signal given by:

$$x(t) = A_1 \cos(\omega_1 t + \phi_1) + A_2 \cos(\omega_2 t + \phi_2) \quad (1)$$

The two tones are at frequencies $\omega_1 = \frac{1}{T_1}$ and $\omega_2 = \frac{1}{T_2}$

(transient simulation), the

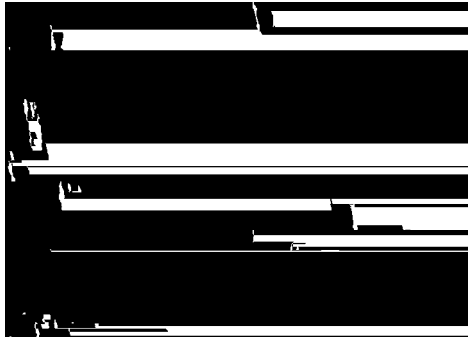
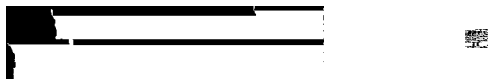


Figure 3: it is a simplistic bivariate representation of FM signal steps taken need to be spaced closely enough that each rapid undulation of $b(t)$ is sampled accurately. If each fast sinusoid is sampled at n

To generate Figure 3

or more are common in electronic circuits.

Now consider the representation obtained as follows: for the ‘fast-varying’ parts, t_1 is replaced by a new variable t_1 ; for the ‘slowly-varying’ parts, by t_2 . The resulting function, now of two variables, is denoted by $f(t_1, t_2)$.



Note that $f(t_1, t_2)$ is periodic with respect to both t_1 and t_2 , i.e., $f(t_1 + T_1, t_2) = f(t_1, t_2)$ and $f(t_1, t_2 + T_2) = f(t_1, t_2)$. The plot of $f(t_1, t_2)$ on the rectangle $0 \leq t_1 < T_1$, $0 \leq t_2 < T_2$ is shown in Figure 2. Because f is bi-periodic, f

Figure 2 was plotted

with 225 samples on a uniform grid

This saving increases with increasing separation of the periods T_1 and T_2 .

Note further that it is easy to recover $f(t)$ from $f(t_1, t_2)$ simply by setting $t_1 = t_2 = t$ and using the fact that f is bi-periodic. Given any value of t , the arguments to f are given by $t_1 = t \bmod T_1$

form can require far fewer samples

are autonomous, frequency-modulation (FM) can be generated. FM cannot, in general, be represented compactly as in Figure 2. We illustrate the difficulty with an example. Consider the following prototypical FM signal

$$f(t) = \cos(2\pi f_1 t + \cos(2\pi f_2 t)) \quad (3)$$

Following the same approach as for (1), a bivariate form can be defined to be

$$f(t_1, t_2) = \cos(2\pi f_1 t_1 + \cos(2\pi f_2 t_2)) \quad (4)$$

Note that $f(t_1, t_2)$ is quasiperiodic with frequencies f_1 and f_2 . Unfortunately, $f(t_1, t_2)$ illustrated in Figure 3, is not a simple surface with only a few undulations like Figure 2. When k

coefficients to capture the undulations.

The WaMPDE approach of this work resolves this problem by bending the path along which f is evaluated away from the diagonal line $t_1 = t_2 = t$. Since along the bent path $t_1 = t_2$ but t_1 is no longer equal to t_2 we refer to t_1 as a warped time-scale. As mentioned in

together with the warping

Note that both $f(t_1, t_2)$ and $f(t)$ can be easily represented with relatively few samples, unlike f in (4). Note further that $f(t)$ is the sum of a linearly increasing term and a periodic term, hence its derivative is periodic. This derivative is equal to the instantaneous frequency, given in (4). For general FM signals (possibly with non-sinusoidal waveforms and varying amplitudes), this derivative, still well-defined, is the derivative of the signal.

To find an efficient bivariate representation, a crucial step in our approach is to avoid specifying the function f a priori, but to impose a smooth ‘phase’ instead on the bivariate function, and use this to calculate

This is accomplished in the following section by the WaMPDE, which is a partial differential equation similar to the MPDE, but with a multiplicative factor of f modifying one of the differential terms. By solving the WaMPDE together with the phase condition mentioned above, compact representations of the solutions of autonomous systems can be found by efficient numerical methods.

4 The Warped Multirate Partial Differential Equation

using vector algebraic equations and many other applications:

$$\frac{d\mathbf{q}}{dt} = \mathbf{f}(\mathbf{q}, \mathbf{b}(t)) \quad (5)$$

In the circuit context, \mathbf{q} is a vector of node voltages and branch currents; $q(t)$ and $i(t)$ are nonlinear functions describing the charge/flux and current terms, respectively. $\mathbf{b}(t)$ is a vector forcing term consisting of inputs, usually independent voltage or current sources.

We now define the two-dimensional WaMPDE to be

$$\frac{\partial f}{\partial t_1} = \mathbf{f}(\mathbf{q}, \mathbf{b}(t_1, t_2))$$

forms for the WaMPDE have been developed of which a special case suffices for the present exposition

With these definitions, it can be shown by substitution that (8) above satisfies (7).

Next, we describe how (8) can be solved to determine $\mathbf{z}(t)$. $\mathbf{z}(t)$ is periodic in t with period T

$$\mathbf{z}(t) = \mathbf{z}(t + T) \quad (9)$$

We note that if $\mathbf{z}(t)$ satisfies (8) then so does for $\mathbf{z}(t + \tau)$ — this is simply because (8) is autonomous in the t time scale. We remove this ambiguity in the same way as for unforced autonomous systems, *i.e.*, by fixing the phase of (say) the z_1 variable to some ϕ_0 , e.g., 0. This is the phase constraint mentioned in Section 3.

We expand (8) in one-dimensional Fourier series in t/T and also include the phase constraint, to obtain:

$$\mathbf{z}(t) = \sum_{k=-\infty}^{\infty} \mathbf{z}_k e^{jk\omega_0 t} \quad (10)$$

\mathbf{O}^f and

series (10) can be truncated to N terms. In the case, N and (10) lead to N equations in the same number of unknown \mathbf{z}_k . Of

Applying periodic or initial boundary conditions to the DAE system (1) and (12) leads to quasiperiodic or envelope-modulated FM solutions, and also captures other interesting phenomena like mode locking and period multiplication. First, we consider periodic boundary conditions.

4.1 Quasiperiodic and envelope solutions

Assume $b(t)$ periodic with period T or angular frequency $\omega_0 = 2\pi/T$. Also assume that the solution of (8) is periodic in both arguments, *i.e.*, $\mathbf{z}(t, \tau)$ and $\mathbf{z}(t, \tau + T)$ can then be written as:

$$\mathbf{z}(t, \tau) = \mathbf{z}_0 + \sum_{k=1}^{\infty} \mathbf{z}_k e^{jk\omega_0 \tau} \quad (11)$$

is a constant, \mathbf{z}_0 is a zero-mean waveform, and its integral \mathbf{z}_0 is a function.

We show by showing that such periodic forms for \mathbf{z}_0 and \mathbf{z}_k capture FM- and AM-quasiperiodicity, locking and period multiplication.

By expressing

$$\mathbf{z}(t, \tau) = \mathbf{z}_0 + \sum_{k=1}^{\infty} \mathbf{z}_k e^{jk\omega_0 \tau} \quad (12)$$

$$\mathbf{z}(t, \tau) = \mathbf{z}_0 + \sum_{k=1}^{\infty} \mathbf{z}_k e^{jk\omega_0 \tau}$$

$p(t)$ is also nontrivially periodic. (15) can then readily be recognized to be a

$$\mathbf{z}(t, \tau) = \mathbf{z}_0 + \sum_{k=1}^{\infty} \mathbf{z}_k e^{jk\omega_0 \tau} \quad (13)$$

axis, covering the interval $[0, T]$. The differentiation operator is replaced by a numerical differentiation formula (e.g., Backward Euler or Trapezoidal), and when the periodic boundary condition $\mathbf{z}(t, \tau) = \mathbf{z}(t, \tau + T)$ is applied, a system of $(N+1)$ nonlinear algebraic equations in $(N+1)$ unknowns is obtained. This set of equations is solved with any numerical method for nonlinear equations, such as

$$\mathbf{z}(t, \tau) = \mathbf{z}_0 + \sum_{k=1}^{\infty} \mathbf{z}_k e^{jk\omega_0 \tau}$$

can be solved for aperiodic

is specified. For typical applications, a natural initial condition is the solution of (7) with no forcing, *i.e.*, with $b(t)$ constant. The procedure for discretizing of the WaMPDE for quasiperiodic or time-stepping solutions is similar to that for the MPDE; further details may be found in

5 Applications

A voltage-controlled oscillator (VCO) was simulated using the new WaMPDE-based numerical techniques. The oscillator consisted of an LC tank in parallel with a nonlinear resistor, whose resistance was negative in a region about zero and positive elsewhere. This led to a stable limit cycle. The capacitance was varied by adjusting the physical plate structure) varactor with a separate control voltage.

The damping parameter of the mechanical structure was initially assumed small, corresponding to a near vacuum.



Figure 4: VCO: frequency modulation

An envelope simulation was conducted using purely time-domain numerical techniques for both t and τ axes. The initial control voltage of V_0 resulted in an initial frequency of about f_0 that of the unforced oscillator.

with the warped τ axis scaled to the oscillator's nominal time-period of T_0 . It is seen that the controlling voltage changes not only the local frequency, but also the amplitude and shape of the oscillator waveform.

The circuit was also simulated by traditional numerical ODE methods ("transient simulation"). The waveform from this simulation, together with the 1-dimensional waveform obtained by applying (9) to Figure 5, are shown in Figure 6. The match is so close that it is difficult to tell the two waveforms apart; however, the thickening of

We used a numerical method: purely



Figure 5: VCO: bivariate representation of capacitor voltage the lines at about 1000 points per nominal cycle, with a resulting speed disadvantage of two orders of magnitude.

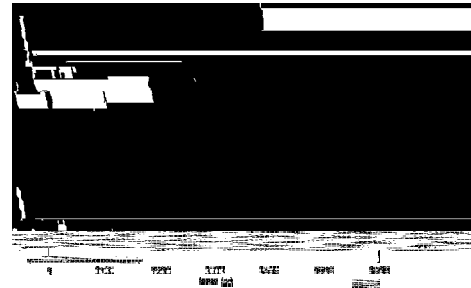


Figure 8: Modified VCO: WaMPDE vs transient (a few cycles at 1000 points per nominal cycle, with a resulting speed disadvantage of two orders of magnitude).

Figure 6: VCO: WaMPDE vs transient simulation

The VCO was simulated again after two modifications: the damping of the MEMS varactor was increased to correspond to an air-filled cavity, and the controlling voltage was varied much more slowly, i.e., about 1000 times slower than the nominal period of the oscillator. The controlling voltage was sinusoidal with a period of 1000. Figure 7 shows the new variation in frequency; note the settling behaviour and the smaller change in frequency, both due to the slow dynamics of the air-filled varactor.



Figure 7: Modified VCO: frequency modulation

The new bivariate capacitor voltage waveform (not shown) was a sinusoid along the warped time scale 1000 but unlike Figure 5, varied very little along the forcing time-scale. This was corroborated by transient simulation, the full results of which are not depicted due to the density of the fast oscillations. A small section of the 1000

Demir, Hans-Georg Brachtendorf, Wim Sweldens and Anirvan Sengupta for discussions of the FM representation problem.

References

1. H.G. Brachtendorf and R. Demir, *Bell Laboratories*, 1996, and A. Sengupta, *signals* 79: 103-112: 1996.
2. M. Demir, *General Internal Document* for Noise Analysis of Large RF Circuits, *IEEE*, Mar 1998.
3. J. Roychowdhury, *Highly Efficient PDE Methods*, *Fund. Methods*, Wiley, 1998.